

RSC Advances



This is an *Accepted Manuscript*, which has been through the Royal Society of Chemistry peer review process and has been accepted for publication.

Accepted Manuscripts are published online shortly after acceptance, before technical editing, formatting and proof reading. Using this free service, authors can make their results available to the community, in citable form, before we publish the edited article. This *Accepted Manuscript* will be replaced by the edited, formatted and paginated article as soon as this is available.

You can find more information about *Accepted Manuscripts* in the [Information for Authors](#).

Please note that technical editing may introduce minor changes to the text and/or graphics, which may alter content. The journal's standard [Terms & Conditions](#) and the [Ethical guidelines](#) still apply. In no event shall the Royal Society of Chemistry be held responsible for any errors or omissions in this *Accepted Manuscript* or any consequences arising from the use of any information it contains.

Ti_{Ga}-V_N complexes in GaN: A new prospect of carrier mediated ferromagnetism

Abdul Majid and Mehreen Javed

Department of Physics, University of Gujrat, Gujrat, Pakistan

Correspondence:

E-mail: abdulmajid40@yahoo.com (Abdul Majid)

Phone: +923328009610

Abstract

First principle investigations, to explore the effects of nitrogen vacancies on ferromagnetism in Ti doped wurtzite GaN, are reported. The presence of nitrogen vacancies demonstrated no noticeable effect in case of pure GaN but exhibited ferromagnetism in case of Ti doped GaN. The magnetic moment however ceased on doubling the concentration of dopant and vacancies in the host which points towards possible antiferromagnetic coupling. The conventional double exchange ordering observed in case of vacancy added Ti:GaN switched to carrier mediated exchange for Ti_{Ga}-V_N complex in Ti:GaN. For Ti doped GaN, the energy difference calculated with and without N vacancy is found relatively smaller than that of other 3d transition metals (Cr, Mn, Fe, Co, Ni, Cu) doped GaN. The results calculated for different configurations to explore the effects of nitrogen vacancies on electronic and magnetic properties of Ti:GaN are discussed in detail.

Keywords

Dilute magnetic semiconductors; Exchange interaction; GaN; Density Functional Theory

1. Introduction

Diluted magnetic semiconductors (DMSs) gained central attention in material science because of their potential for applications in future appliances. These materials are realized by introducing magnetic dopants in conventional semiconductors and have attracted intense interest due to their prospective use in developing novel magneto-electronic, magneto-optical and specially

spintronic devices that utilizes both the charge and spin character of electrons to create new functionalities [1-3]. After Ohno's discovery of carrier induced ferromagnetism in initial DMS material Mn:GaAs that exhibited a critical temperature of 110 K, numerous experimental and theoretical studies appeared reporting room temperature magnetic ordering in II-VI, III-V, and IV-VI DMSs [4]. Dietl predicted that wide bandgap semiconductors are good candidates for obtaining room temperature ferromagnetism and voted in favor of GaN:Mn [5]. Owing to the development of sophisticated growth techniques the scope of material science is expanding and the searching curve of suitable DMS materials is at its peak.

Though GaN has been extensively studied for its exceptional electronic and optoelectronic properties but its potential for use in magnetic random access memory (MRAM), spin light emitting diodes (spin LEDs), spin field effect transistors (FETs), spin based quantum dots, magnetic tunnel junctions and other storage elements opened new research areas [6]. The doping of GaN matrix with transition metals (TMs), bearing partial occupancy of d-orbitals, is an effective method to realize nitride based DMSs [7-10]. The induced ferromagnetism roots from magnetic exchange interaction as explained by several models including double exchange, p-d exchange, super-exchange, bound magnetic polaron and carrier mediated interaction. The carrier mediated interaction is held by interaction between magnetic impurities and propagating charge carriers in the host. These carriers are generated as a result of native defects in form of vacancies, interstitials and antisites that may control many aspects of DMS, particularly FM, by significant variations in their carrier's densities [11].

In earlier 1990's, vacancies, the most prevalent and inevitable native point defects, found in both cationic and anionic sublattices of bulk GaN, have been examined in numerous theoretical studies [7-13]. Anionic Nitrogen vacancies typically behave as shallow donors and are reported to be a dominant defect in GaN to show its n-type conductivity [14] while cationic gallium vacancies act as acceptors [15] and have been found to induce a local magnetic moment [16]. Pratibha Dev *et. al.* suggested that neutral cation vacancy in GaN leads to strong localization of defect states favoring spontaneous spin polarization and formation of local magnetic moment. The extended tails of defect wave functions, on the other hand, mediate surprisingly long-range magnetic interactions between the defect-induced moments [17]. Zhihua Xiong *et. al.* also proposed that ferromagnetism in GaN is due to Ga vacancy whereas N vacancy induces no magnetism [18]. It was found that the room-temperature ferromagnetism of undoped GaN

nanoparticles [19] originates from the ferromagnetic spins coupling of Nitrogen dangling bonds associated with the surface Ga-vacancies through bond spin polarization and is effective even when vacancy separation is as long as 8 Å. Latter, in 2010, in GaN thin films and nanowires ferromagnetism driven by cation vacancy study by Anlong Kuanga *et. al.* suggested that magnetic moments mainly come from the unpaired 2p electrons at nearest-neighbor N atoms of the Ga vacancy [20]. In 2011, the experimental evidence of Ga-vacancy induced room temperature ferromagnetic behavior in GaN films, by using plasma-assisted molecular beam epitaxy reported the experimental evidence of room temperature ferromagnetism, believed to originate from the polarization of the unpaired 2p electrons of N surrounding the Ga vacancy [21]. Earlier investigations mainly focused that considerable amounts of native defects only argued for cationic Ga sites in as-grown GaN [17-21] but recently theoretical study [22] established that the Nitrogen vacancy should also serve as a dominant defect in GaN. Recently, it has been indicated that disability of V_{Ga} to induce room temperature ferromagnetism corresponding to a Curie temperature of 150 K at the density lower than that value $1.28 \times 10^{21} \text{ cm}^{-3}$ concentration [23]. Instead of frequently studied cationic sublattice vacancies, in the field of defect induced ferromagnetism in semiconductors, other anionic sublattice vacancy induced magnetism, is still controversial as cationic nitrogen-vacancy in pure GaN causes no spin polarization but when introduced in presence of impurity it induces magnetic moment [18].

There are many materials studied yet indicating this novel way of ferromagnetism assisted by introducing anionic vacancy in doped semiconductors as in (Be, Mg)-GaN (2003) [24], magnetic ions-TiO₂ (2007) [25], Ti-ZnO [26], Mn-GaN films [27], Mn-SrTiO₃ [28], Co-Dy₂O₃ [29]. Recently the effects of Nitrogen vacancies on 3d-transition metals including Cr, Mn, Fe, Co, Ni and Cu in GaN [30] was studied however literature still lacks the Ti-doped GaN study in context of anionic defect induced ferromagnetism although it may prove very important in prospect as Ti favorably replaces Ga in Ti⁺³ form ultimately left with one unpaired electron thus offering high flexibility to study the effect of N vacancy in magnetic interaction variation. Ti for being an important nonmagnetic dopant responsible to induce favorable ferromagnetism is studied in host environment of ZnO [31, 32], AlN [33], AlP [34], GaN [35]. Being motivated by growing interest in innovative defect-impurity states induced ferromagnetism, here a detailed study in framework of anionic nitrogen vacancy effects on Ti-GaN is presented.

2. Computational details

The first-principles calculations based on density functional theory were performed on pure and Ti doped bulk wurtzite GaN using supercell approach implemented in Amsterdam density functional (ADF) BAND package [35]. All calculations were carried out on 32 atoms supercells.

The first part of calculations was devoted to pure GaN in the form of (a) defect free GaN with unit cell formula $\text{Ga}_{16}\text{N}_{16}$ and (b) with nitrogen vacancy defect denoted by unit cell formula $\text{Ga}_{16}\text{V}_\text{N}\text{N}_{15}$. The second part of the calculations deals with doping of Ti on cationic sites of GaN in the form of Ti_{Ga} with and without nitrogen vacancy represented by unit cell formulae of $\text{Ga}_{15}\text{Ti}_1\text{V}_\text{N}\text{N}_{15}$ and $\text{Ga}_{15}\text{Ti}_1\text{N}_{16}$ respectively, where V_N symbolizes the absence of single nitrogen atoms on anionic site of the matrix. The calculations were also carried out for two Ti atoms doped GaN without vacancy in the form of supercell $\text{Ti}_2\text{Ga}_{14}\text{N}_{16}$ ($\text{Ga}_{14}\text{N}_{16}+2\text{Ti}_{\text{Ga}}$) and with two vacancies in the form of supercell $\text{Ti}_2\text{Ga}_{14}\text{N}_{14}$ ($\text{Ga}_{15}\text{N}_{15}+2\text{V}_\text{N}+2\text{Ti}_{\text{Ga}}$).

The calculations were performed using generalized gradient approximation (GGA) based on Perdew-Burke-Ernzerhof (PBE) functional as it is found very accurate to theoretically investigate electric and magnetic properties of DMSs [36-39]. However there exist an inevitable limitation of GGA functional to properly describe the magnetic properties of TMs doped compounds, therefore; to improve the calculation we included on-site d-d Coulomb interaction by adding Hubbard U parameter to GGA. Hence this work also includes the comparative study of Ti-doped GaN using GGA and GGA+U. The value of Hubbard U was considered as $U=4.5$ eV and $J=0.5$ eV in agreement with the literature [40-43]. For self-consistent field (SCF) convergence the basis set of linear combination of atomic orbitals (LCAO) with Triple zeta double polarization (LCAO+Tz2P) was utilized. All the configurations of wurtzite GaN were fully relaxed and geometrically optimized, using the experimental lattice constants of $a=3.189\text{\AA}$ and $c=5.185\text{\AA}$ and internal parameter 0.377 as starting parameters [44]. The cutoff energy was found 1.00×10^{-4} eV. The Brillouin zone integration was performed by using Γ -centered k-point grid with $2\times 2\times 2$ Monkhorst Pack Mesh.

TM preferably substitute cationic substitutional site in compound semiconductors as it offers relatively low formation energy, hence we considered dopant in the form of Ti_{Ga} [45]. The vacancy is introduced at anionic N site; denoted V_N ; that usually introduces shallow donor levels in materials [46, 47]. The orbitals per electronic configurations used in the calculations Ga [$4s^2$,

$3d^{10}$, $4p^1$], N [$2s^2$, $2p^2$] and Ti [$4s^2$, $3d^2$] were taken as valence while rest of inner electrons were kept frozen.

3. Results and Discussions

The density of states (DOS) calculated for series of geometrically optimized structures of GaN, in pure and Ti doped form, were discussed in detail to explore the potentials of the material for carrier mediated ferromagnetism. The following sections describes our findings to explain the effects of nitrogen vacancies on structural, electronic and magnetic properties on Ti doped GaN.

A. Structural properties of the configurations studied

One of the objectives of this study was to explore the likelihood of formation of complex $Ti_{Ga}-V_N$ in GaN matrix where V_N was introduced at the nearest-neighbor position of Ti_{Ga} , at a distance of 1.948\AA . In case of Mn:GaN, the complex $Mn_{Ga}-V_N$ has been experimentally pointed out as one of the stable defects in GaN; as Mn prefers to sit on Ga lattice site at place close to vacant N site [48,49]. Moreover, this configuration keeps the separation between V_N and Ti_{Ga} less than 3.00\AA which is appropriate to allow the conspicuous interaction of defect's wave functions to cause the defect induced ferromagnetism [50]. The results indicated that geometrically optimized configurations of GaN supercell with V_N or Ti_{Ga} are considerably fluctuated from the starting lattice parameters. The optimized lattice parameters for all studied supercells are listed in Table 1 whereas figure 1 shows the supercell highlighting the positions of the dopant and vacancy.

Table 1: Lattice parameters and positions of defects in GaN supercell for all configurations

Configuration	a (\AA)	c (\AA)	Location per Fig.1	
			V_N	Ti_{Ga}
1. $Ga_{16}N_{16}$	3.186	5.186	--	--
2. $Ga_{16}N_{15}(Ga_{16}N_{16}+V_N)$	3.067	5.100	1	--
3. $Ti_1Ga_{15}N_{16}(Ga_{15}N_{16}+Ti_{Ga})$	3.176	5.176	--	3
4. $Ti_2Ga_{14}N_{16}(Ga_{14}N_{16}+2Ti_{Ga})$	3.149	5.163	--	3,4
5. $Ti_1Ga_{15}N_{15}(Ga_{15}N_{15}+V_N+Ti_{Ga})$	3.002	5.040	1	3
6. $Ti_2Ga_{14}N_{14}(Ga_{15}N_{15}+2V_N+2Ti_{Ga})$	2.840	4.891	1,2	3,4

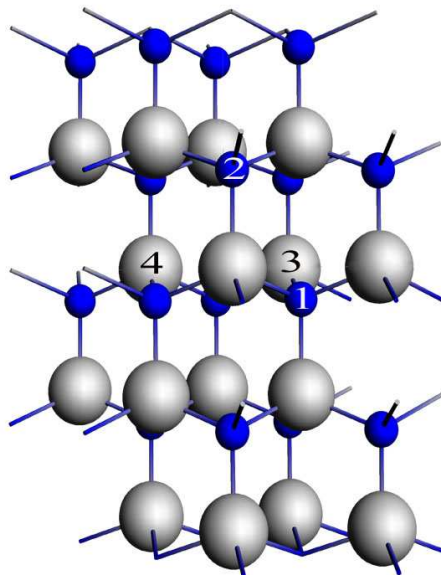


Fig. 1: wurtzite bulk GaN supercell showing locations of substituted dopants (Ti_{Ga}) and nitrogen vacancies (V_{N}) labeled as 3,4 and 1,2 sites respectively.

The observed gradual decrease in $d_{\text{Ga-Ga}}$ along a- and c-axes on introduction and increment of the defects may be attributed to variant fashion of bonding between fused atoms as the radius of Ga is 2.050 Å, Ti is 1.992 Å and N is 1.608 Å. The distance between two interacting atoms should be roughly equal to the sum of their surface radii, therefore; keeping radii into account it can be said that in current situation of Ti:GaN the bond length decreases as per expectation when compared with GaN. The reduction of the lattice dimensions is caused by the inter-ionic coulomb interactions due to partly ionic nature of the material [51]. The relaxed geometries of supercells of the configurations used for this study are given in figure 2.

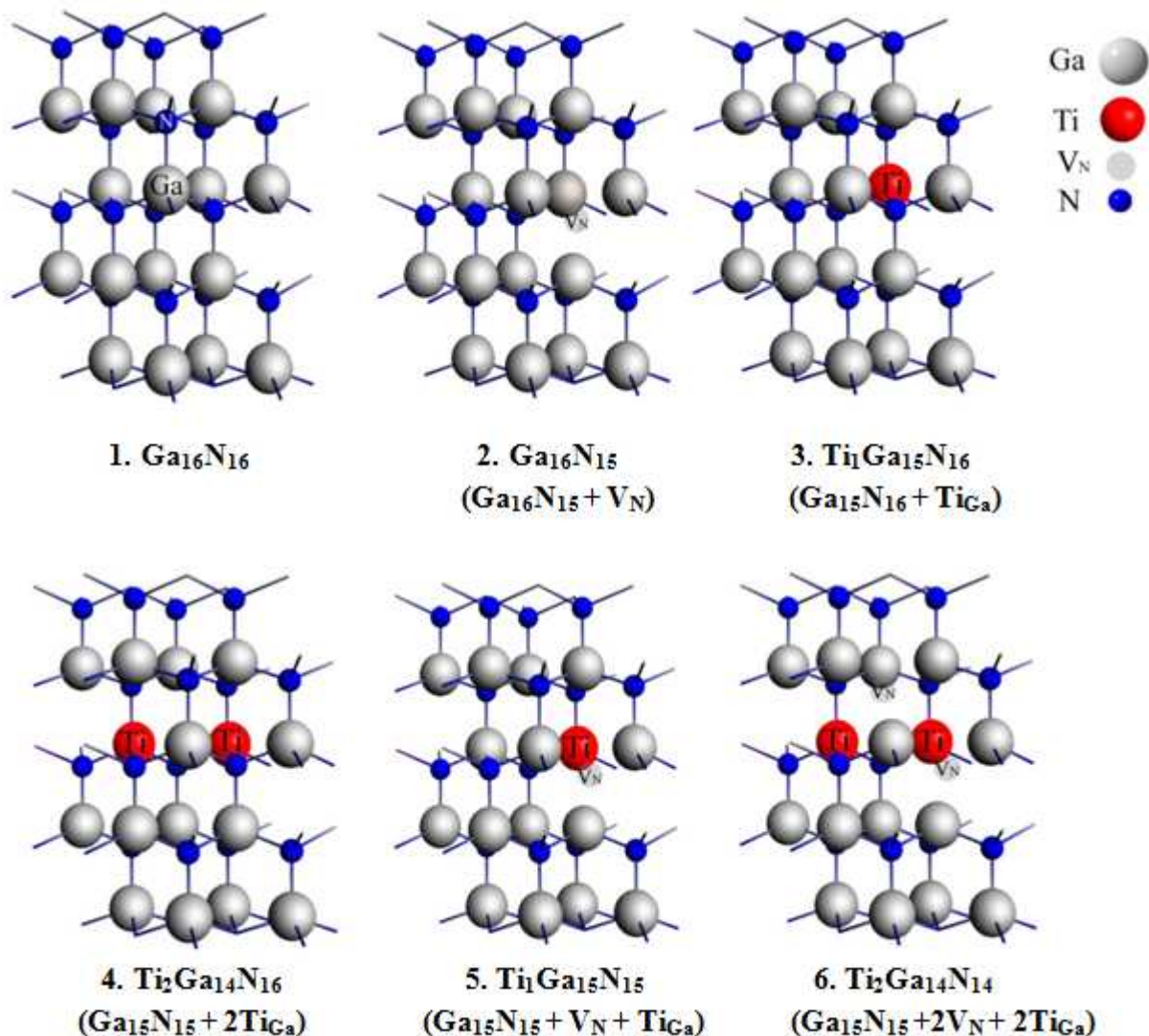


Fig. 2: Geometrically optimized supercell structures of the configurations studied.

In order to study the role of nitrogen vacancies and $\text{Ti}_{\text{Ga}}-\text{V}_\text{N}$ complex in ferromagnetic ordering of $\text{Ti}:\text{GaN}$, we carried out detailed calculations on different configurations such as pure GaN , single V_N in GaN , single and double Ti_{Ga} in GaN and pair of $\text{Ti}_{\text{Ga}}-\text{V}_\text{N}$ complexes. The values of Fermi energy, formation energy and magnetic moment calculated for different configurations are described in table II.

Table II: The calculated values of energies and magnetic moment for different configurations

Configuration	Fermi energy: E_F GGA (GGA+U)	Formation Energy: E_f GGA (GGA+U)	Magnetic moment per supercell GGA (GGA+U)	Magnetic moment per Dopant/Vacancy GGA (GGA+U)

	eV	eV	μ_B	μ_B
$\text{Ga}_{16}\text{N}_{16}$	-5.74	-24.85	0.00	0.00
$\text{Ga}_{16}\text{V}_N\text{N}_{15}$	21.55	-186.47	0.00	0.00
$\text{Ga}_{15}\text{Ti}_1\text{N}_{16}$	17.28 (18.45)	-200.45 (-194.09)	-1.00 (-1.00)	-0.98 (-1.14)
$\text{Ga}_{15}\text{Ti}_1\text{V}_N\text{N}_{15}$	19.00 (21.04)	-191.53 (-185.38)	0.882 (1.97)	0.58 (1.83)
$\Delta E = E(\text{vac}) - E(\text{no vac})$	1.72 (2.59)	8.92 (8.71)	--	--
$\Delta\mu = \mu(\text{vac}) - \mu(\text{no vac})$	--	--	1.88 (2.97)	1.56 (2.97)

B. Properties of Ti:GaN

The configuration $\text{Ga}_{15}\text{Ti}_1\text{N}_{15}$ has lowest formation energy pointing towards solubility of Ti in GaN matrix. Furthermore, Fermi level shifted towards conduction band with vacancy introduction which predicts n-type nature of GaN. Figure 3 gives DOS for $\text{Ga}_{15}\text{Ti}_1\text{N}_{16}$ representing single Ti atom substitutionally placed on cationic site of GaN without vacancy. The results (calculated with GGA) depict the dominance of spin polarized Ti-3d impurity band system near Fermi energy level at CBM pointing towards possible ferromagnetic ordering. However, by switching on the Hubbard U correction, the self-interaction correction caused the delocalization of *d*-states thereby providing an inverted hump near band gap mid, in agreement with Mn:GaN structure. The inversion corresponds to conventional spin down state of singly occupying Ti-3d electrons [57, 58].

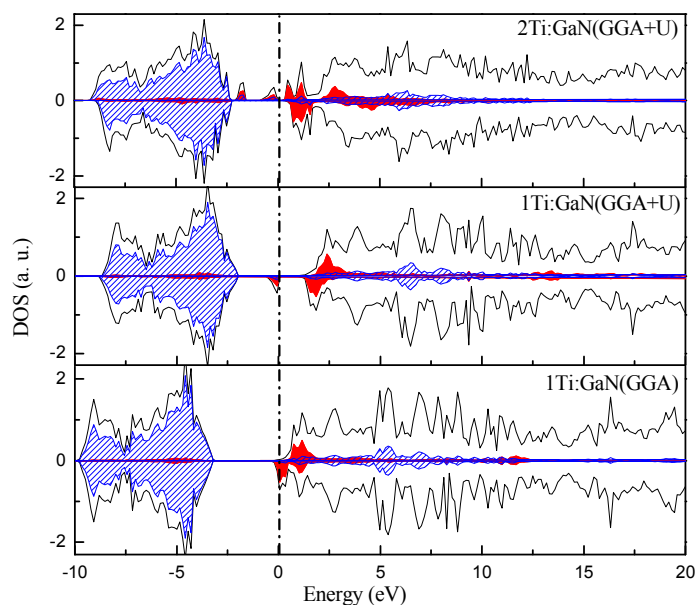


Fig. 3: The DOS plots for $(\text{Ga}_{15}\text{Ti}_1\text{N}_{16})$ and $(\text{Ga}_{14}\text{Ti}_2\text{N}_{16})$ where total density of states (TDOS) is represented by the solid line while blue shaded area represents the partial density of states (PDOS) of N-2p and red shaded represents Ti-3d states

In order to investigate the magnetic coupling between Ti atoms we performed calculations on two Ti_{Ga} atoms substitutionally doped in form of supercell $\text{Ti}_2\text{Ga}_{14}\text{N}_{16}$ using GGA+U. The ferromagnetic (FM) state is found stable for being lower in energy than antiferromagnetic (AFM) state in agreement with Z. Xiong [35]. The induced ferromagnetism with a magnetic moment of $2.00 \mu_{\text{B}}$ is calculated for $\text{Ti}_2\text{Ga}_{14}\text{N}_{16}$ configuration having Ti-dopants introduced at nearest neighboring positions. The spin polarized TDOS plots for $\text{Ti}_1\text{Ga}_{15}\text{N}_{16}$ and $\text{Ti}_2\text{Ga}_{14}\text{N}_{16}$ display half metallic behavior (HMB) of the material representing these configurations. This ordering is due to p-d exchange interactions caused by hybridization between the Ti-3d majority spin components and N-2p band. It allows electron hopping between Ti 3d states through intermediary N-2p orbitals thus aligning all 3d electrons in ferromagnetic order via double exchange mechanism in agreement with observations of several DMS materials like Ti:ZnO [31,32], Ti:AlN [33], V: GaN [60] etc. The comparative view of TDOS for $\text{Ga}_{14}\text{Ti}_2\text{N}_{16}$ with Ti-3d and N-2p PDOS distinctly highlights 3d-2p hybridization to assist the exchange interactions. In order to comprehend magnetic ordering in $\text{Ti}_1\text{Ga}_{15}\text{N}_{15}$, TDOS and PDOS plots for $\text{TiGa}_{15}\text{N}_{15}$ are shown in fig. 4.

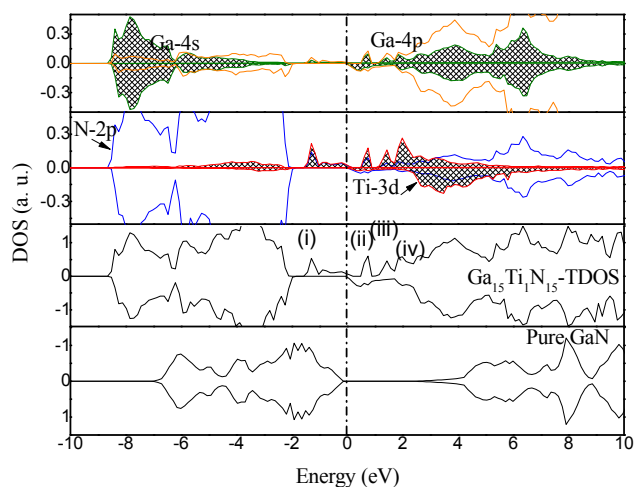


Fig. 4: The TDOS plots for $(\text{Ga}_{15}\text{Ti}_1\text{N}_{15})$ with N-2p, Ga-4p, Ga-4s and Ti-3d orbitals PDOS in comparison with pure GaN. Ti 3d and Ga 4s states are shown shaded.

C. Properties of Ti:GaN with single nitrogen vacancy

To shed light on the influence of nitrogen vacancies on electronic structure of Ti-doped GaN the plots of calculated total and partial density of states were analyzed. The comparison of DOS indicates that the introduction of nitrogen vacancy into GaN (as $\text{Ga}_{16}\text{N}_{15}+\text{V}_\text{N}$) causes reduction of bond length $d_{\text{Ga-Ga}}$ along c-axis from 5.186 Å to 5.100 Å and along a-axis from 3.186 Å to 3.067 Å. Besides the structural changes, other material properties were also observed to change notably on incorporation of nitrogen vacancies in GaN matrix. V_N introduces fairly shallow donor levels in the bottom of conduction band and causes shift of Fermi energy level towards the bottom edge of conduction band which indicates intrinsic n-type nature for GaN in line with literature [46, 54]. The observation of partial DOS shows that occupied CBM states comes mainly from Ga-4p and Ga-4s dangling bonds formed due to N vacancy. The reduction of $d_{\text{Ga-Ga}}$ along a- and c-axes, causes increased bonding trend between first neighboring Ga atoms around the V_N lattice site due to far more extended donor states in agreement with earlier studies [55-56].

In order to reveal the influence of the N vacancies on the magnetic properties of Ti:GaN the calculated values of magnetic moments for different configurations with and without vacancy are given in table II. The difference of the magnetic moments per dopant per supercell with and without N vacancy is notable. It has been observed that value of magnetic moments per supercell and per TM-ions is independent on the sites of the vacancies [30]. Similar to the cases of Mn:GaN [27] and Cr:GaN [50], the magnetic moment of Ti:GaN is observed to increase in the presence of V_N , but its value is comparatively smaller than that of Cr and Mn doped GaN cases whereas fairly larger than that of Fe, Co, Ni, and Cu-doped GaN systems [30].

The results indicated that nitrogen vacancies enhances magnetic moment in Ti:GaN. In order to model the situation, it should be useful to have a look into the electronic structure of the host and the way dopant is accommodated. In GaN, which is unintentionally n-doped, nitrogen vacancy is a shallow donor and is an established cause of providing electrons to the conduction band [14]. Like other TMs Ti substitutes cationic Ga-sites in form of Ti^{+3} in GaN [52, 53]. The available states in Ti^{3+} -3d¹ fivefold orbitals are occupied by additional electrons, in spin-up alignment, released from dangling bonds in the vicinity of nitrogen vacancies. It causes an increase in magnetic moment from its expected value of $1\mu_\text{B}$ per dopant ion in agreement with cases of Mn- and Cr-doped GaN containing single V_N [27, 50]. The enhanced ferromagnetism

also agrees with the magnetic behavior of Cr: AlN [30] and Ti: ZnO [31, 32] in the presence of N and O vacancies respectively. On the opposite footing in case of Fe^{3+} , Co^{3+} , Ni^{3+} , or Cu^{3+} the extra available electrons occupy spin-down states after occupation of spin-up states in five d orbitals. This explains the probable cause of reduction of magnetic moment in TM ions (having filled spin-up band) doped GaN with nitrogen vacancies when compared with the similar case of Ti:GaN [30].

From table II; it is interesting to note that the credit of increased magnetic moment in $\text{Ga}_{15}\text{Ti}_1\text{N}_{15}$ configurations when compared with $\text{Ga}_{15}\text{Ti}_1\text{N}_{16}$ goes to V_N . As without vacancy, for $\text{Ga}_{15}\text{Ti}_1\text{N}_{16}$ configuration, Ti contributes major part to total magnetic moment of supercell as compared to $\text{Ga}_{15}\text{Ti}_1\text{N}_V\text{N}_{15}$ configuration where although Ti constitutes relatively smaller part but rest of the contribution comes from introduced nitrogen vacancy. Both GGA and GGA+U calculations support it.

D. Properties of $\text{Ti}_{\text{Ga}}\text{-}V_N$ complex in Ti:GaN

After discussing the electronic structures for pure $\text{Ga}_{16}\text{N}_{16}$, $\text{Ga}_{16}\text{N}_{15}$ ($\text{Ga}_{16}\text{N}_{16}+V_N$), $\text{TiGa}_{15}\text{N}_{16}$ ($\text{Ga}_{15}\text{N}_{16}+\text{Ti}_{\text{Ga}}$) and $\text{Ti}_2\text{Ga}_{14}\text{N}_{16}$ ($\text{Ga}_{14}\text{N}_{16}+2\text{Ti}_{\text{Ga}}$), in the following section we describe the central configuration of our calculation, $\text{Ti}_1\text{Ga}_{15}\text{N}_{15}$ ($\text{Ga}_{15}\text{N}_{15}+\text{Ti}_{\text{Ga}}+V_N$), forming $\text{Ti}_{\text{Ga}}\text{-}V_N$ complex. The DOS plots calculated on configuration $\text{Ga}_{15}\text{Ti}_1\text{N}_{15}+V_N$ using GGA and GGA+U for $\text{Ti}_{\text{Ga}}\text{-}V_N$ complex are shown in figure 5. The introduction of nitrogen vacancy show a significant change in electronic structure of Ti:GaN as V_N induces states resonant with impurity band formed near Fermi level at the bottom of the conduction band. The bottom of VB is mainly formed by N-2s, with minor contribution from Ga-4s and Ga-4p. The top of VB comprises with major contribution from N-2p and minor part from Ga-4p, Ga-4s and N-2s. The bottom edge of CB consists of Ti-3d, N-2p, Ga-4p, Ga-4s whereas top of CB consists mainly of Ga-4p. This spin polarized impurity band involves a major contribution from Ti 3d orbitals and exhibits half metallic behavior. This trend of half metallicity is more pronounced with GGA+U calculation. Obviously p-d exchange interactions resulting from hybridization between Ti-3d and N-2p band in the vicinity of the Fermi level should be responsible for the induced ferromagnetism like in previously discussed systems. The only difference now is simultaneous presence of V_N which provides free carriers. The observed overlap of Ti 3d states with V_N related donor states near Fermi level predicts the transfer of carriers from surroundings of nitrogen vacancies to the Ti-3d

band that enhances the local magnetic moment per Ti ions to cause carrier mediated exchange interactions.

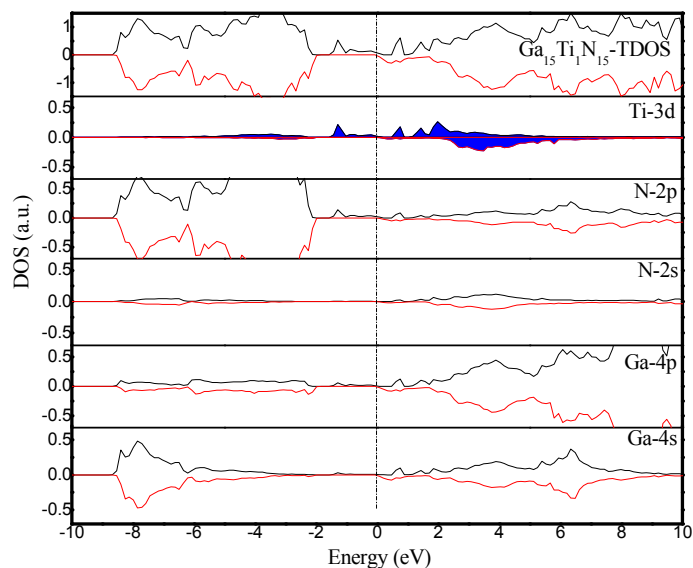


Fig. 5: The TDOS plots for $\text{Ti}_{\text{Ga}}\text{-V}_{\text{N}}$ complex ($\text{Ga}_{15}\text{Ti}_1\text{N}_{15}$) in comparison with N-2p, N-2s, Ga-4p, Ga-4s and Ti-3d orbitals PDOS with GGA+U. Ti 3d states are shown shaded.

On inclusion of nitrogen vacancy near Ti_{Ga} the formation of complex $\text{Ti}_{\text{Ga}}\text{-V}_{\text{N}}$ is likely which, when checked through DFT calculations in the form of the configuration $\text{Ga}_{15}\text{Ti}_1\text{V}_{\text{N}}\text{N}_{15}$, appeared as most stable arrangement. This finding is consistent with the reported experimental finding that Mn prefers to substitute the Ga sites closest to nitrogen vacancies [49]. Though formation energy with vacancy is comparatively higher but this configuration presents higher magnetic moment pointing towards its significance for DMS materials. The role of vacancies in ferromagnetic ordering and exchange interactions in case of TM doped compound semiconductors has been extensively studied and reported [31, 32]. The difference in values of formation energy calculated with and without V_{N} for TM-doped GaN is 8.92 eV (8.71 eV) using GGA (GGA+U) that is interestingly smaller than the reported values for other TM doped GaN as Cr (10.21 eV), Mn (9.78 eV), Fe (10.73 eV), Co (9.07 eV), Ni (9.60 eV) and Cu (9.19 eV) [30]. It points towards highest likelihood of presence of Ti_{Ga} near anionic vacancy that favors formation of $\text{Ti}_{\text{Ga}}\text{-V}_{\text{N}}$ complex in Ti:GaN.

The GGA+U calculated value of magnetic moment per Ti for $\text{Ga}_{15}\text{Ti}_1\text{N}_{16}$ is $1 \mu_B$ whereas its value for $\text{Ti}_{\text{Ga}}\text{-V}_{\text{N}}$ complex is $1.97\mu_B$. The increase in magnetic moment is dedicated to vacancy introduction thus predicting the role of nitrogen vacancies to enhance ferromagnetism in Ti doped GaN. This result is in accordance with a recent report by Zhenzhen Weng in which they considered the anionic O vacancy increases the magnetic moments of Ti-doped ZnO [26]. For $\text{TiGa}_{15}\text{N}_{15}$, the formation of four humps near Fermi level (Fig. 3) may help to describe this increased ferromagnetic behavior in Ti doped GaN in the case of $\text{Ti}_{\text{Ga}}\text{-V}_{\text{N}}$ complex. A hybridization between impurity derived Ti-3d states (having major contribution of 3d xz, yz, zx antibonding orbitals) and V_{N} derived donor states (having major contribution of Ga-4p, Ga-4s and N-2p) is evident. It is observed that first hump involves the hybridization between Ti-3d (xz) and N-2p, second hump involves the hybridization between Ti-3d (xz), Ga-4p and Ga-4s, third hump involves the hybridization between Ti-3d (xy) and Ga-4p whereas the fourth hump involves the hybridization between Ti-3d (yz), Ga-4p and Ga-4s states. The charge transfer across these hybridized states by itinerant electrons supports a carrier mediated interaction to establish a long range magnetic order. The carrier mediated interaction is a function of dopant-vacancy distance therefore in order to strengthen the exchange interaction it is suggested to introduce nitrogen vacancy in nearest neighbor site of the dopant in Ti:GaN. The hybridization of Ti-3d and Ga-4p dangling states near the Fermi level and charge transfer from the donor derived band to unoccupied Ti-3d states supports a long-range magnetic ordering between Ti ions via the itinerant electrons.

E. Properties of Ti:GaN with double nitrogen vacancy

To further study the prospects of $\text{Ti}_{\text{Ga}}\text{-V}_{\text{N}}$ complexes in GaN, we studied another configuration of $\text{Ti}_2\text{Ga}_{14}\text{N}_{14}$ ($\text{Ga}_{14}\text{N}_{14}+2\text{Ti}_{\text{Ga}}+2\text{V}_{\text{N}}$), thereby doubling the concentration of nitrogen vacancies, in order to further explore the characteristic of nitrogen vacancies in Ti doped GaN. It was very interesting to know that magnetic moment becomes zero which points to the information that on doubling the concentration of V_{N} the long range magnetic exchange interaction between substitutional Ti dopants extinguishes. This high Ti doping concentration in Ga rich environment appears to arrange the dopants in antiferromagnetic ordering in the matrix.

It is suggested to the material growers to optimize the ammonia flow rate in order to avoid the nitrogen deficient atmosphere which may cause the harmful effects on ferromagnetic

spin coupling between two nearest substitutional Ti atoms in Ti:GaN diluted magnetic semiconductor. The suitably optimized growth conditions may provide driving force to bring foreign Ti atoms to substitute cationically near nitrogen vacancy to set up $\text{Ti}_{\text{Ga}}\text{-V}_{\text{N}}$ complex in the material. It will be a stable complex and enhance the ferromagnetism as V_{N} acts as donor and Ti_{Ga} acts as acceptor. It is therefore recommended to enhance the N partial pressure to reduce the appearance of N vacancy, avoiding the destruction of ferromagnetic coupling between the Ti atoms by the vacancies.

A long-range magnetic coupling is critical for achieving high temperature magnetism at low defect concentrations. The results suggest that $\text{Ti}_{\text{Ga}}\text{-V}_{\text{N}}$ complex supports long range magnetic interaction in favor of carrier mediated ferromagnetism [60]. Ultimately this intrinsic defect derived and impurity facilitated long-range magnetic coupling hosted at low defect concentrations opens a new route toward designing high T_c DMS according to $k_{\text{B}}T_c=2\Delta E/3c$ where c is the concentration of dopant. The comparative view of TDOS plots for all considered configuration is shown in figure 6.

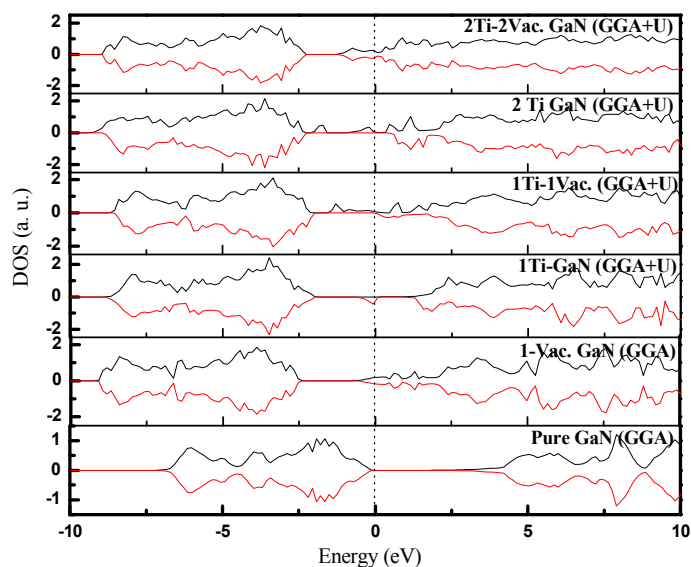


Fig. 6: The TDOS plots for all considered configurations

Conclusions:

It is concluded that pure GaN demonstrates absence of magnetic moment but it becomes spin polarized by Ti doping. The un-doped GaN with single V_{N} is again non-spin-polarized however it reveals n-type conductivity which becomes more pronounced at high vacancy concentration.

However, upon simultaneous incorporation of Ti (on cationic site) and V_N on neighboring sites in GaN matrix to realize $Ti_{Ga}-V_N$, a pronounced increase in magnetic moment is observed. On the other hand, upon doubling the Ti and V_N concentration in same supercell, magnetic moment became zero which is possibly due to antiferromagnetic coupling between dopants. It is therefore recommended that crystal growers should enhance the nitrogen partial pressure to limit the appearance of N vacancies that triggers AFM coupling in Ti:GaN. The hybridization of dopant and host states causes transfer of charge from the donor derived band to unoccupied Ti-3d states which supports a long-range magnetic ordering between Ti ions via the itinerant electrons. The carrier mediated interaction is a function of dopant-vacancy distance therefore it is suggested that nitrogen vacancy may be introduced in nearest neighbor site of the dopant in order to strengthen the exchange interaction in Ti:GaN.

References:

- [1] N. Newman, S. Y. Wu, H. X. Liu, J. Medvedeva, L. Gu, R. K. Singh, Z. G. Yu, I. L. Krainy, S. Krishnamurthy, D. J. Smith, A. J. Freeman and M. Van Schilfgaarde, *Phys. Stat. Sol. (a)*, 2006, **203**, 2729-2737
- [2] N. S. Rogado, J. Li, A. W. Sleight and M. A. Subramanian, *Adv. Mater.*, 2005, **17**, 2225-2227
- [3] D. D. Awschalom and M. E. Flatte, *Nat. Phys.*, 2007, **3**, 153-159
- [4] F. Matsukara, H. Ohno and T. Dietl, *Handbook of Magnetic Materials*, Elsevier, Amsterdam, 2002, **14**, 1-87
- [5] T. Dietl, H. Ohno, F. Matsukura, J. Cibert and D. Ferrand, *Science*, 2000, **287**, 1019-1022
- [6] Ferrand, D.; Wasiele, A.; Tatarenko, S.; Cibert, J.; Richter, G.; Grabs, P.; Schmidt, G.; Molenkamp, L. W.; Dietl, T., *Solid State Communications*, 2001, **119**, 237-244
- [7] J. Neugebauer and C. G. Van de Walle, *Phys. Rev. B*, 1994, **50**, 8067-8070
- [8] P. Boguslawski, E. L. Briggs and J. Bernholc, *Phys. Rev. B*, 1995, **51**, 17255-17258
- [9] C. H. Park and D. J. Chadi, *Phys. Rev. B*, 1997, **55**, 12995-13001

- [10] T. Mattila and R. M. Nieminen, *Phys. Rev. B.*, 1997, **55**, 9571-9576
- [11] K. Sato *et al.*, *Rev. of Mod. Phys.*, 2010, **82**, 1633-1690
- [12] I. Gorczyca, A. Svane and N. E. Christensen, *Phys. Rev. B.*, 1999, **60**, 8147-8157
- [13] C. G. Van de Walle and J. Neugebauer, *J. Appl. Phys.*, 2004, **95**, 3851-3879
- [14] M. G. Ganchenkova and R. M. Nieminen, *Phys. Rev. Lett.*, 2006, **96**, 196402
- [15] A. Gulans, R. A. Evarestov, I. Tale and C. C. Yang, *Phy. Stat. Sol. (c)*, 2005, **2**, 507-510
- [16] J. Hong, *J. Appl. Phys.*, 2008, **103**, 63907
- [17] P. Dev, Y. Xue, and P. Zhang, *Phys. Rev. Lett.*, 2008, **100**, 117204-117206
- [18] Z. Xiong, L. Luo, J. Peng and G. Liu, *J. Phy. Chem. Sol.*, 2009, **70**, 1223-5
- [19] H. Jin, Y. Dai, B. B. Huang and M. H. Whangbo, *Appl. Phy. Lett.*, 2009, **94**, 162505
- [20] A. Kuanga, H. Yuana and Hong Chena, *App. Sur. Sci.*, 2010, **256**, 6040-6046
- [21] B. Roul, M. K. Rajpalke, T. N. Bhat, M. Kumar, A. T. Kalghatgi and S. B. Krupanidhi, *Appl. Phy. Lett.*, 2011, **99**, 162512
- [22] X. Wang, M. Zhao, T. He, Z. Wang and X. Liu, *App. Phy. Lett.*, 2013, **102**, 062411
- [23] C.D. Latham, R. Jones, S.O. berg, R.M. Nieminen and P.R. Briddon, *Phy. Rev. B.*, 2003, **68**, 205209
- [24] G. Cohen, V. Fleurov and K. Kikoin, *J. Appl. Phys.*, 2007, **101**, 09H106
- [25] Z. Weng, Z. Huang and W. Lin, *Physica B*, 2012, **407**, 743-747
- [26] B. Hu, B.Y. Man, M. Liu, C. Yang, C.S. Chen, X.G. Gao, S.C. Xu, C.C. Wang, Z.C. Sun, *Appl Phys A.*, 2012, **108**, 409-413
- [27] S. Middey, C. Meneghini, and S. Ray, *Appl. Phy. Lett.*, 2012, **101**, 42406
- [28] A. Bandyopadhyay, S. Sutradhar, B.J. Sarkar, A.K. Deb and P.K. Chakrabart, *Appl. Phy. Lett.*, 2012, **100**, 252411
- [29] B. Xu and B.C. Pan, *J. Appl. Phys.*, 2009, **105**, 103710
- [30] J. Zhang, X. Z. Li, B. Xu, and D. J. Sellmyer, *Appl. Phys. Lett.*, 2005, **86**, 212504
- [31] G. Yao, G. Fan, H. Xing, S. Zheng, J. Maa, S. Li, Y. Zhang and M. He, *Chem. Phy. Lett.*, 2012, **529**, 35-38
- [32] Z. Xiong, F Jiang, *J. Phy. Chem. Sol.*, 2007, **68**, 1500-1503
- [33] S.W. Fan, K.L. Yao, Z.G. Huang, J. Zhang, G.Y. Gao and G.H. Dua, *Chem. Phy. Lett.*, 2009, **482**, 62-65
- [34] P. Liang, Y. Liu, X.H. Hu, L. Wang and Q. Dong, *J. Magn. Mag. Mat.*, 2014, **355**, 295-299
- [35] Z. Xiong, S. Shi and F. Jiang, *Chem. Phy. lett.*, 2007, **443**, 92-94
- [36] G.T. Velde, F.M. Bickelhaupt, E.J. Baerends, C.F. Guerra, S.J.A. Van Gisbergen, J.G. Snijders and T. Ziegler, *J. Comp. Chem.*, 2001, **22**, 931-967
- [37] J.P. Perdew, K. Burke and M. Ernzerhof, *Phys. Rev. Lett.*, 1996, **77**, 3865

- [38] P. Hohenberg and W. Kohn, *Phys. Rev. B*, 1964, **136**, 864
- [39] W. Kohn and L. Sham, *Phys. Rev. Lett.*, 1965, **14**, 1133
- [40] V. I. Anisimov, J. Zaanen and O. K. Andersen, *Phys. Rev. B*, 1991, **44**, 943
- [41] W. E. Pickett, S. C. Erwin and E. C. Ethridge, *Phys. Rev. B*, 1998, **58**, 1201
- [42] M. Cococcioni and S.D. Gironcoli, *Phys. Rev. B*, 2005, **71**, 35105
- [43] P. Gopal and N. A. Spaldin, *Phys. Rev. B*, 2006, **74**, 94418
- [44] N. Tandon, G. P. Das and A. Kshirsagar, *Phys. Rev. B*, 2008, **77**, 205206
- [45] J.A. Chisholm and P.D. Bristowe, *Modelling Simul. Mater. Sci. Eng.*, 2001, **9**, 249-258
- [46] D.C. Reynolds, Z.Q. Fang, J.W. Hemsley, J.R. Sizelove and R.L. Jones, *Mat. Sci. Eng. B.*, 1999, **66**, 30-32
- [47] J.O. Guillen, S. Lany, S.V. Barabash and A. Zunger, *Phys. Rev. Lett.*, 2006, **96**, 107203
- [48] Z.Z. Weng, J.M. Zhang, Z.G. Huang and W.X. Lin, *Chin. Phys. B*, 2011, **20**, 27103
- [49] D.J. Keavney, S.H. Cheung, S.T. King, M. Weinert and L. Li, *Phys. Rev. Lett.*, 2005, **95**, 257201
- [50] Y. Li, W. Fan, H. Sun, X. Cheng, P. Li, X. Zhao and M. Jiang, *J. Solid State Chem.*, 2010, **183**, 2662-2668
- [51] R.D. Shannon, *Acta Crystallogr.*, 1976, **32**, 751- 767
- [52] X.Y. Cui, J.E. Medvedeva, B. Delley, A.J. Freeman, C. Stampfl, *Phys. Rev. B*, 2007, **76**, 45201
- [53] D. Heiman, M. Dahl, X. Wang, P.A. Wolff, P. Becla, A. Petrou and A. Mycielski, *Mater. Res. Soc. Symp. Proc.*, 1990, **161**, 479
- [54] A. Majid, W. Akram and A. Dar, *Comp. Mat. Sci.*, 2014, **88**, 71-75
- [55] A. Fara, F. Bernardini and V. Fiorentini, *J. Appl. Phys.*, 2001, **85**, 1999
- [56] K. Laaksonen, M.G. Ganchenkova and R.M. Nieminen, *J. Phys. Condens. Matter.*, 2009, **21**, 015803
- [57] L.M. Sandratskii, P. Bruno and J. Kudrnovsky, *Phys. Rev. B.*, 2004, **69**, 195203
- [58] F. Zhou, M. Cococcioni, C.A. Marianetti, D. Morgan and G. Ceder, *Phy. Rev. B*, 2004, **70**, 235121
- [59] Guangrui Yao , Guanghan Fan , Haiying Xing , Shuwen Zheng , Jiahong Ma, Shutu Li ,Yong Zhang, Miao He, *Chem. Phy. Lett.*, 2012, **529**, 35-38
- [60] J. Osorio-Guill'en, S. Lany, S.V. Barabash, and A. Zunger, *Phys. Rev. Lett.*, 2006, **96**, 107203